Properties of the ionized gas in HH objects in Orion: Results from integral field spectroscopy with PMAS

Mesa-Delgado, A (IAC)
López-Martín, L (IAC)
Esteban, C (IAC)
García-Rojas, J (IAC)
Luridiana, V (IAC)
Núñez-Díaz, M (IAC)

HH objects in Orion: Results from PMAS

Introduction

Observations

Line Measurements and Reddening Correction

Physical conditions

Chemical abundances

Temperature fluctuations

Correlations ADF and other nebular properties

Conclusions

L. López-Martín

HH objects in Orion: Results from PMAS

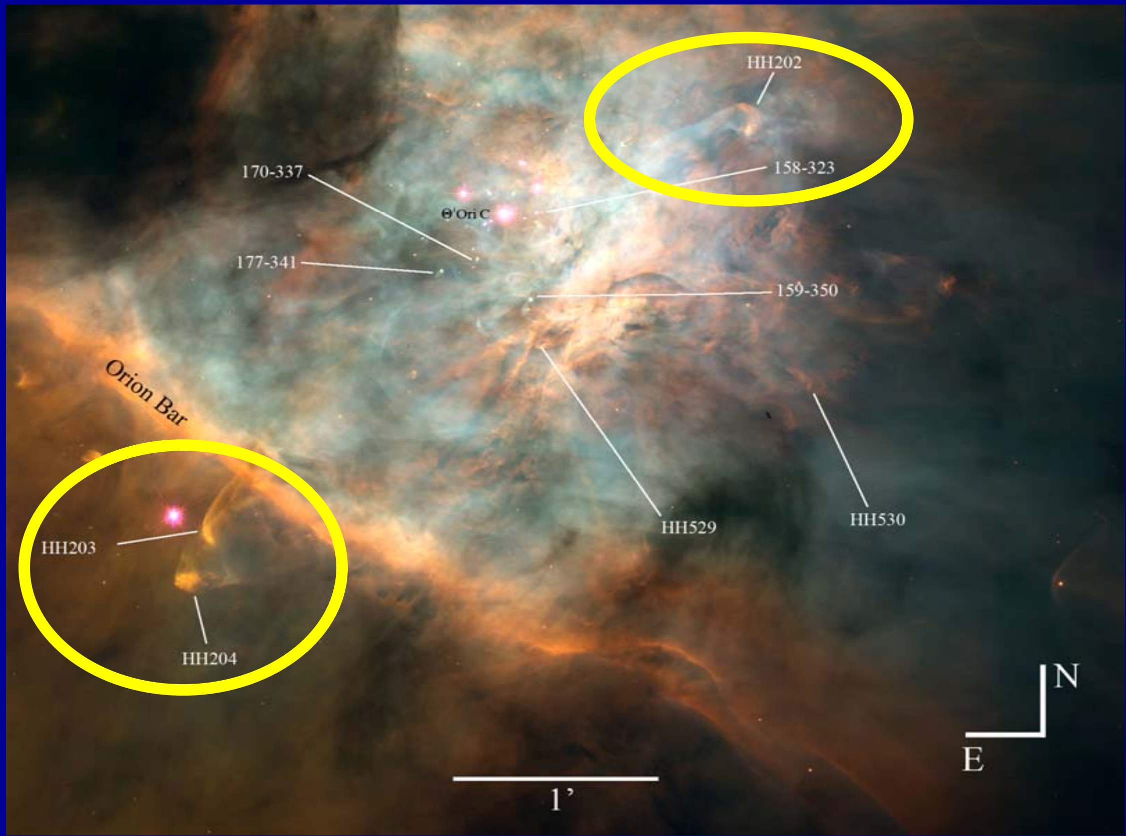

O'Dell & Wong 1996

O'Dell et al. (1997) with *HST* → detailed imaging study of Orion in the [SII], [OIII] and Hα

extended → HH202 photoionized

Chemical composition (specially AD)

Esteban et al. (1998)
Esteban et al. (2004)
Mesa-Delgado, Esteban & García-Rojas (2008)

Spatial distribution physical properties

O'Dell, Peimbert & Peimbert (2003) HST images
Rubin et al. (2003) STIS
Sánchez et al. (2007) PPAK
Mesa-Delgado, Esteban & García-Rojas (2008) ISIS

Orion Sánchez et al. (2007) PPAK
Tsamis, Walsh & Pécquignot (2009) FLAMES
Mesa-Delgado et al. (2009) PMAS
Nuñez-Díaz et al. (2009) in prep. PMAS

HH objects in Orion: Results from PMAS

Observations

HH 202 2007 October at CAHA (Almería,Spain)
HH 203 & HH204 2008 December at CAHA (Almería,Spain)

IFU of 16 x 16 arcsec^2 FOV

V600 grating
- Rotating angle -72 3500-5100 Å
- Rotating angle -68 5700-7200 Å

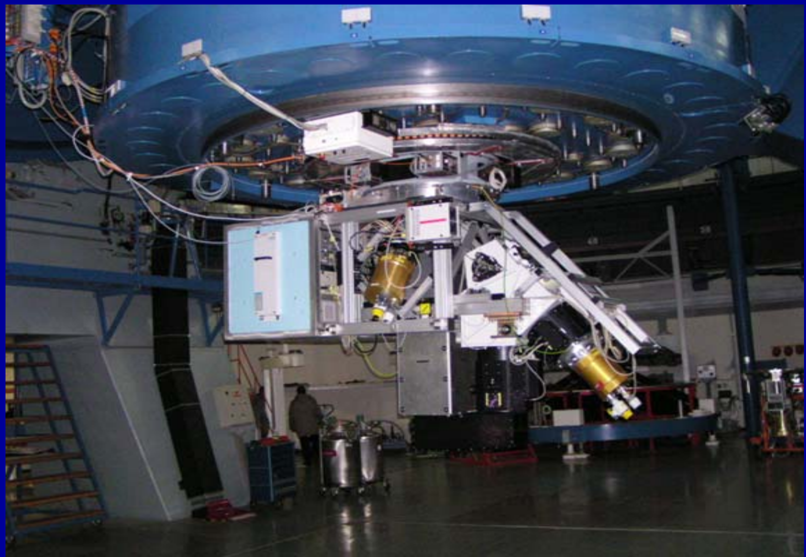

PMAS* at CAHA 3.5m

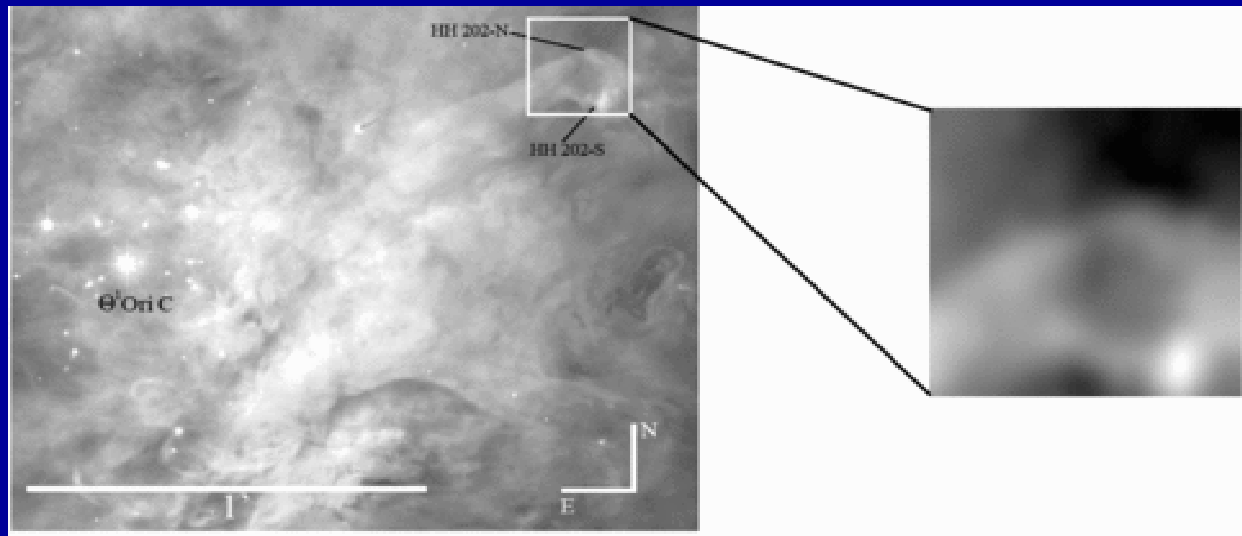

HST image of the central part of the Orion Nebula (O'Dell & Wong 1996).

Reduced using the IRAF reduction package SPECRED

* Roth et al. 2005, PASP, 117,832

HH objects in Orion: Results from PMAS

Line Measurements and Reddening Correction

The emission lines considered:

a) Balmer Lines, from Hα to H11

b) CELs of various species (physical conditions and ionic abundances)

c) Faint RLs of CII and OII (ionic abundance and ADF)

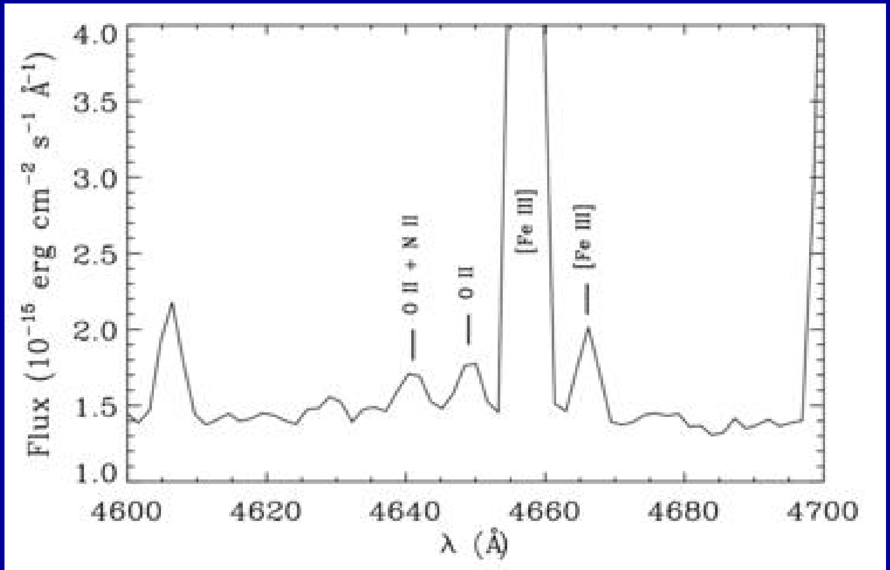

Section of a PMAS spectrum of HH 202 around OII lines of multiplet

L. López-Martín

HH objects in Orion: Results from PMAS

Line Measurements and Reddening Correction

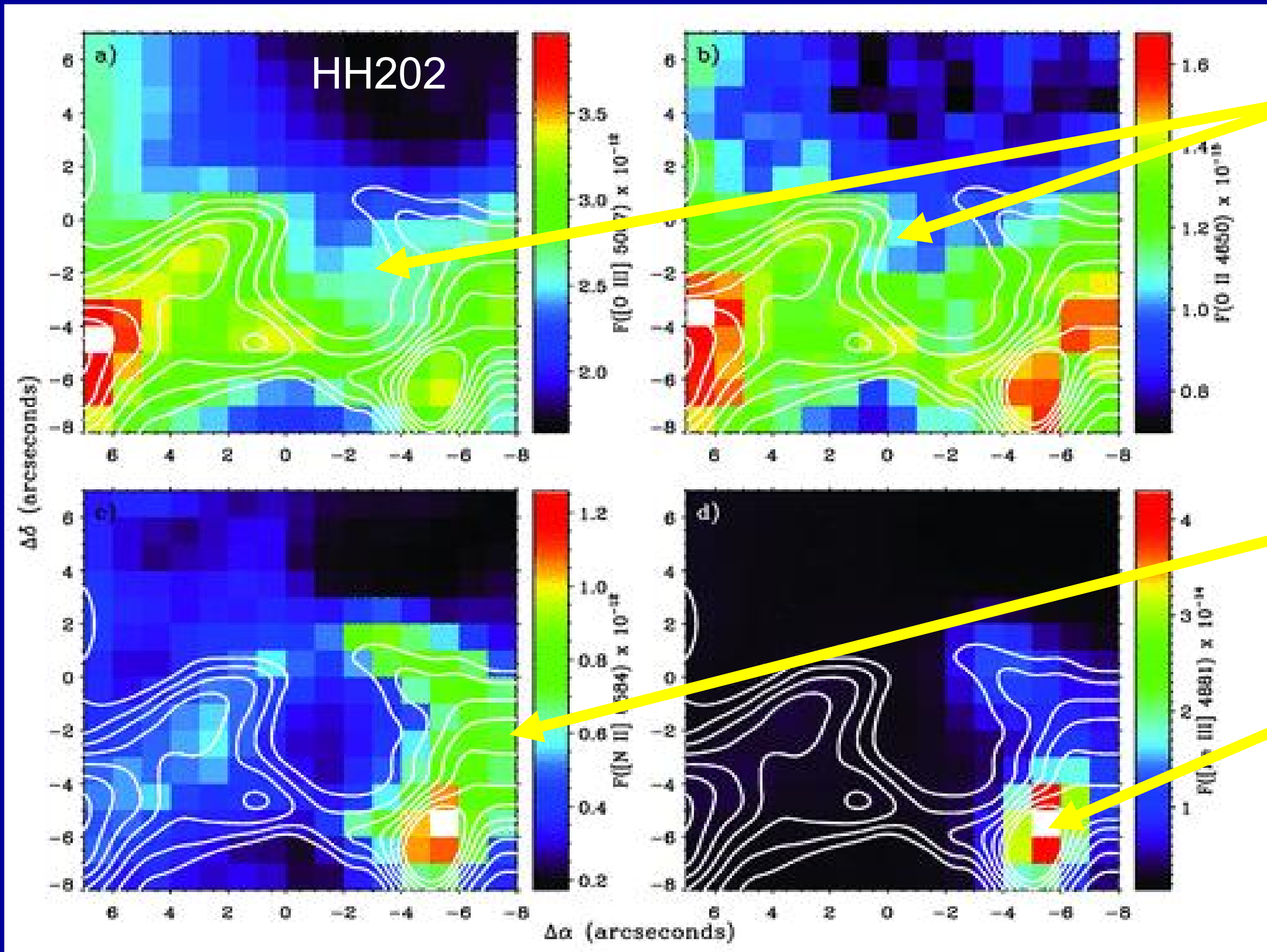

[OIIII] 5007 and OII 4650 quite similar

[NII] enhancement in the bow shock

[FeIII] concentrated at HH 202-S

HH objects in Orion: Results from PMAS

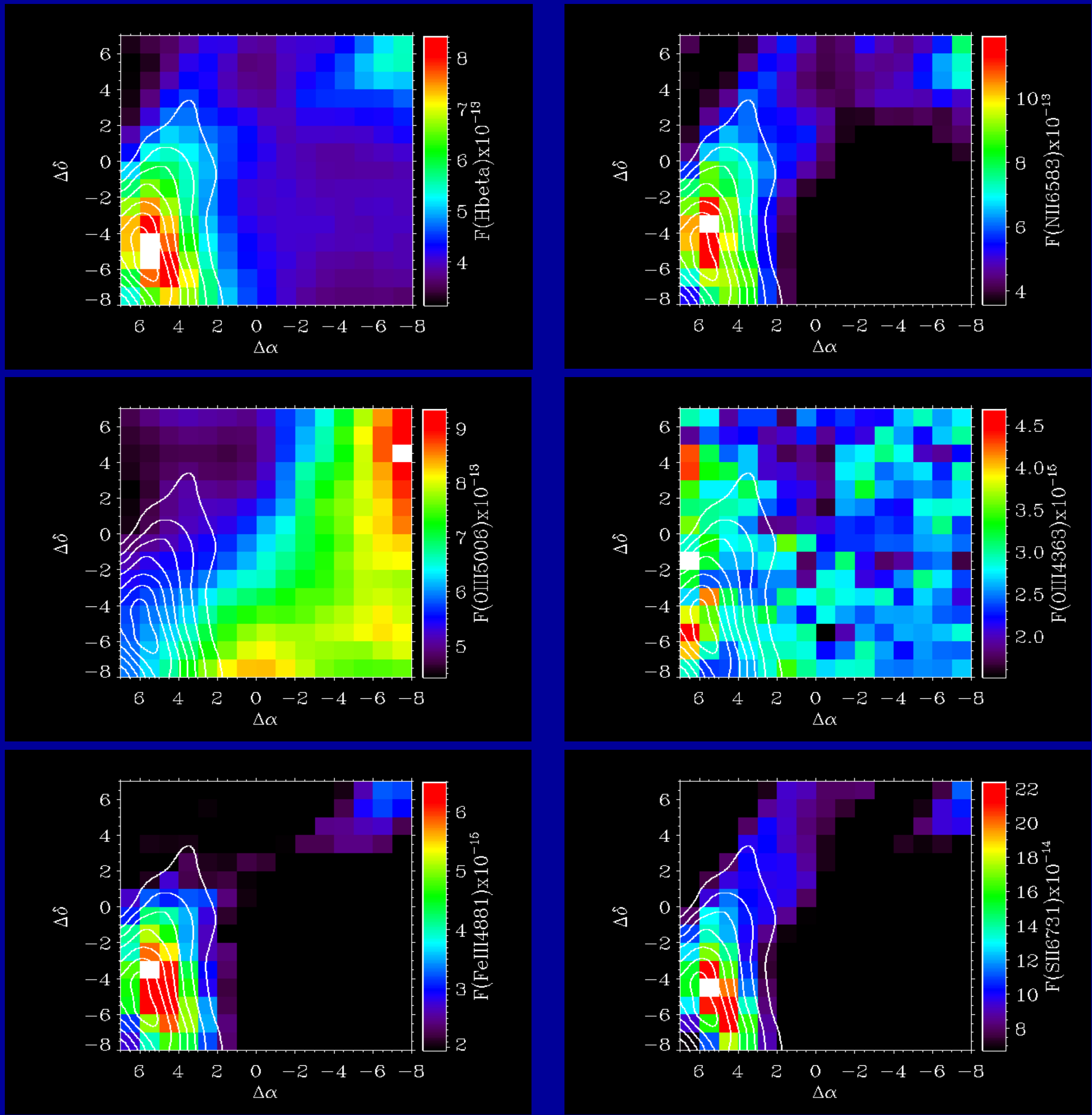

HH 203

L. López-Martín

HH objects in Orion: Results from PMAS

HH 204

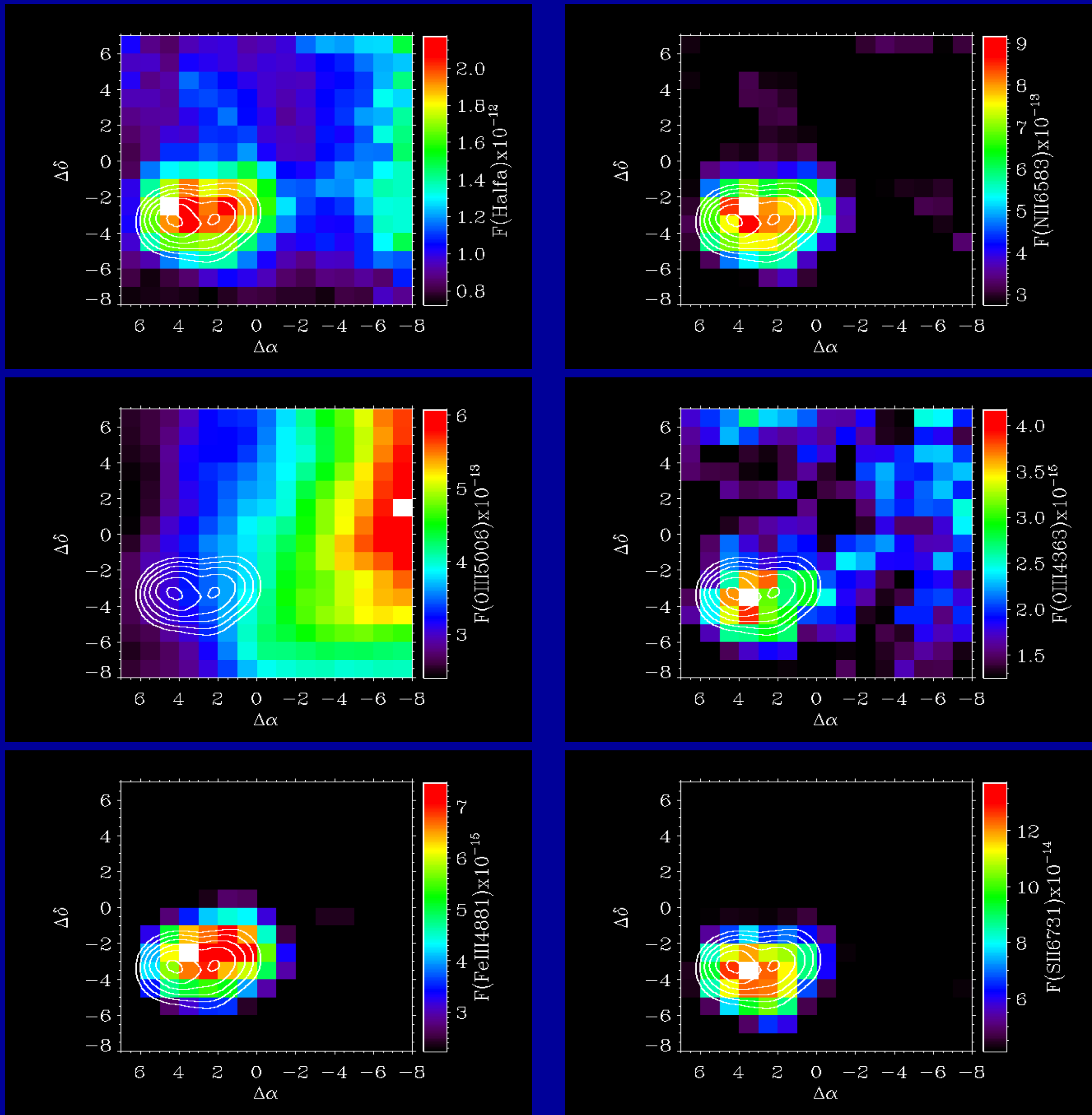

L. López-Martín

HH objects in Orion: Results from PMAS

Line Measurements and Reddening Correction

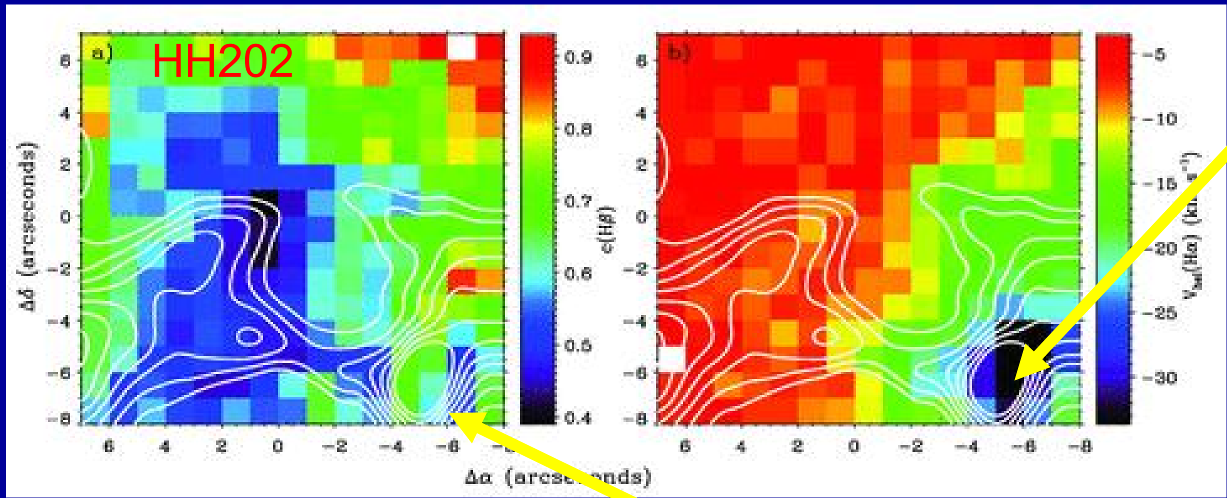

Doi et al. (2004) -39±2 km s^{-1}

Hγ /Hβ , Hδ /Hβ ,H9/Hβ & H11/Hβ ~ Storey & Hammer (1995)
Reddening function Blagrave et al. (2007) for Orion nebula

O'Dell & Yusef-Zadech (2000) from Hα /Hβ HST & radio to optical surface brightness ratio → 0.2-0.4

Mesa-Delgado et al. (2008) from long slit spectroscopy → 0.4±0.1

L. López-Martín

HH objects in Orion: Results from PMAS

Physical conditions

n_e ~10000 cm^{-3} (Mesa-Delgado et al. 2008)

n_e → [SII] 6717/6731

Te → [OIII] (4959+5007)/4363
[NII] (6548+6584)5755

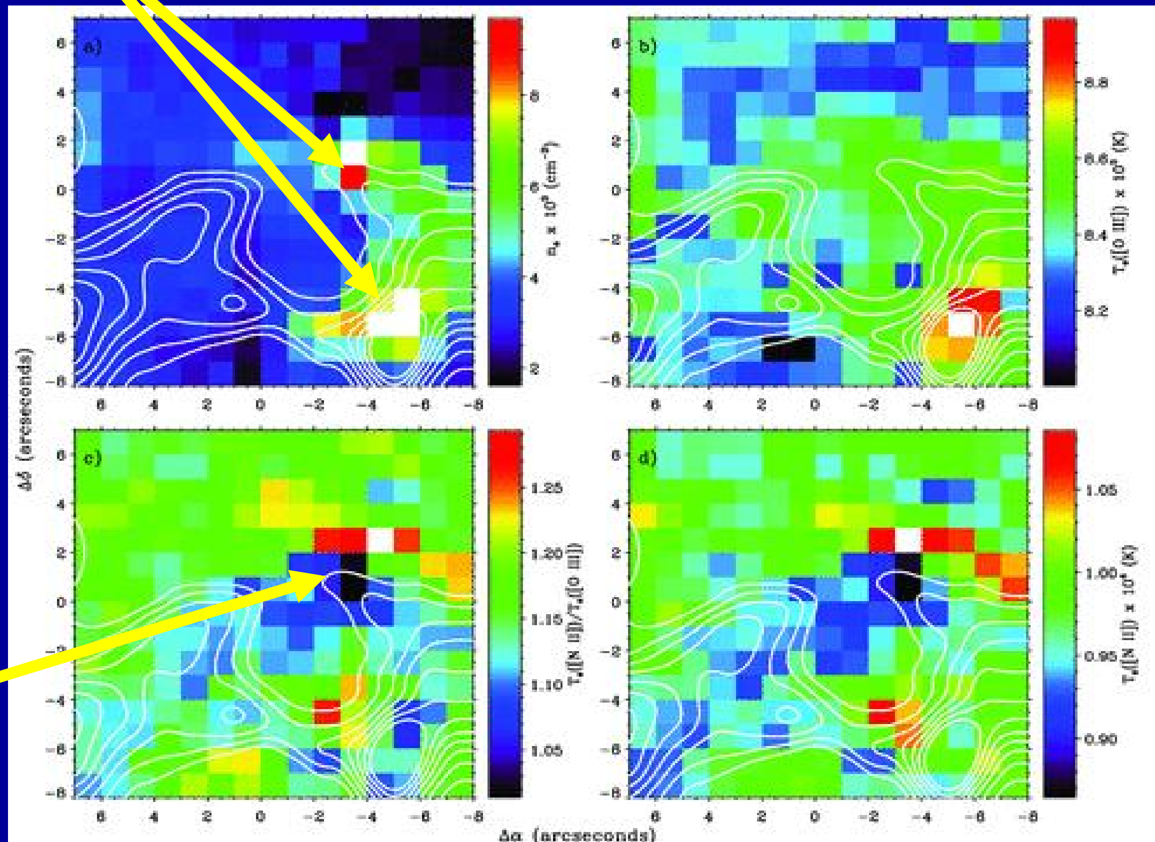

T_e [NII] >T_e [OIII] ~1 HH202_N

HH objects in Orion: Results from PMAS

Physical conditions

$$T_e(\mathrm{Bac}) = 368\left(1 + 0.259y^{+} + 3.409y^{2+}\right)\left(\frac{\mathrm{BJ}}{\mathrm{H11}}\right)^{-(3/2)}$$

Liu et al. (2001)

y^{+} Esteban et al. (2004)
y^{2+} =0 (lack of Helium II lines)

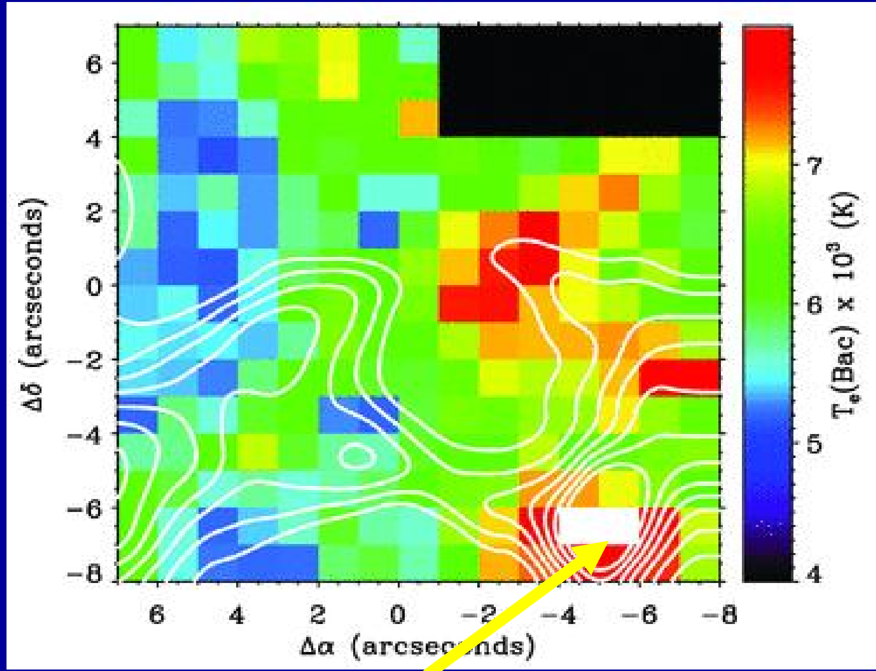

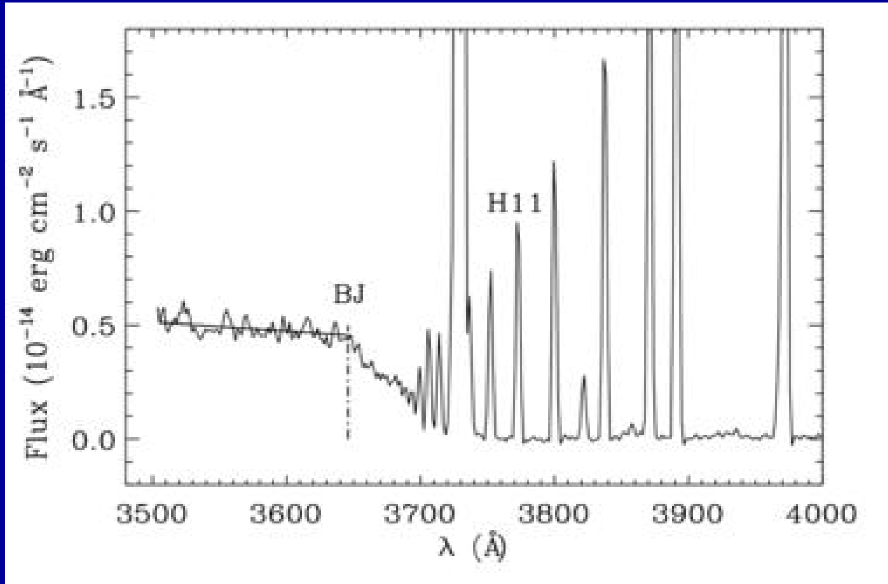

PMAS spectrum at the apex (-5.5,-6.5) spaxel

T_e (Bac) similar distribution T_e [OIII]
Maximum values HH202-N and HH202-S

HH objects in Orion: Results from PMAS

Chemical abundances

Ionic abundances of N^{+} , O^{+} and O^{2+} from CELs

Ionic abundances of O^{2+} and C^{2+} from RLs

O^{2+}/H^{+} minimum
O^{+}/H^{+} maximum
} Different ionization structure

N^{+} very similar to O^{+}

OII 4649 and 4651 +

$$\left[\frac{I(4651+74)}{I(\mathrm{sum})}\right]_{obs} = 0.101 + \frac{0.128 \pm 0.010}{[1+N_e(\mathrm{FL})/2800]}$$

$$\left[\frac{I(4649)}{I(\mathrm{sum})}\right]_{obs} = 0.397 - \frac{0.269 \pm 0.010}{[1+N_e(\mathrm{FL})/2800]}$$

Peimbert & Peimbert (2005)

⇓

I(M1 OII)/ I(Hβ)

+

$$\frac{\mathrm{O}^{2+}}{\mathrm{H}^{+}} = \frac{\lambda_{\mathrm{M1}}}{4861}\,\frac{\alpha_{\mathrm{eff}}(\mathrm{H}\beta)}{\alpha_{\mathrm{eff}}(\mathrm{M1})}\,\frac{I(\mathrm{M1\,O\,II})}{I(\mathrm{H}\beta)}$$

⇓

O^{2+} / H^{+}

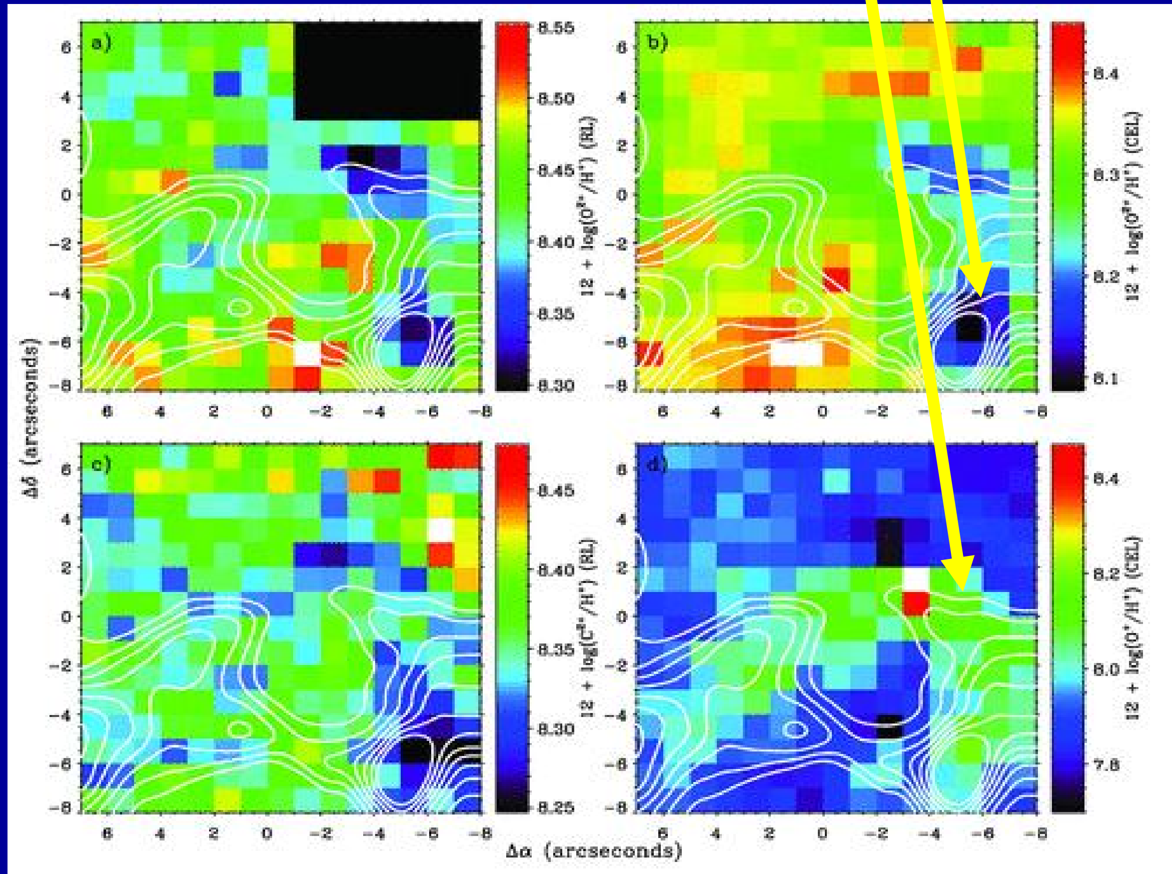

L. López-Martín

HH objects in Orion: Results from PMAS

Chemical abundances

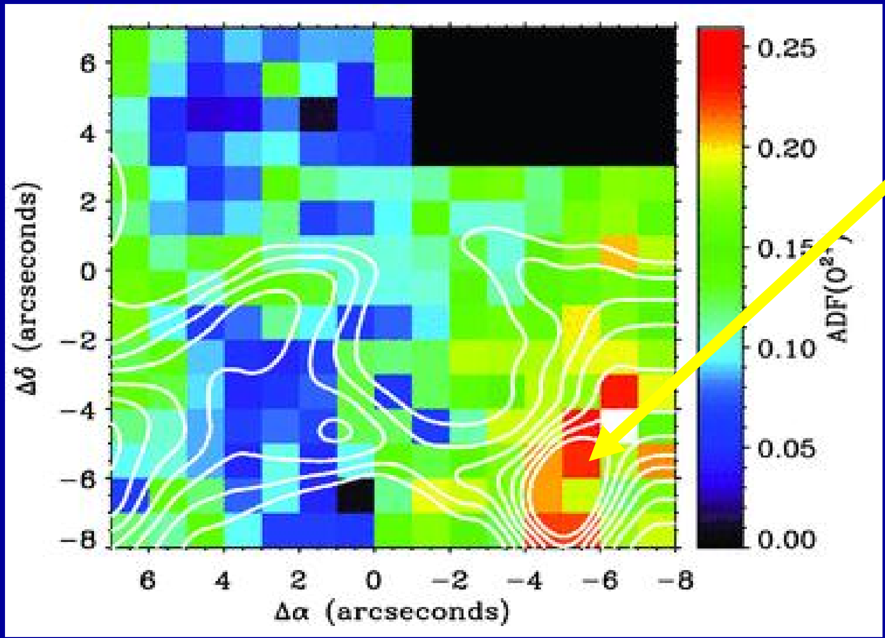

max ADF(O^{2+}) ~0.23 dex HH202-S

Mesa-Delgado et al. (2008) ~0.30 dex

<ADF(O^{2+})> 0.13 ± 0.05 dex

HH objects in Orion: Results from PMAS

Temperature fluctuations

Explanation for the AD problem in ionized nebula

$$T_0 = \frac{\int T_e n_e n_i \, dV}{\int n_e n_i \, dV} \qquad t^2 = \frac{\int (T_e - T_0)^2 n_e n_i \, dV}{T_0^2 \int n_e n_i \, dV}$$

Peimbert (1967)

Several methods t^2:

1) compare T_e obtained from independent methods

$$T_e(\mathrm{Bac}) = T_0(1 - 1.70 t^2)$$

Peimbert (1967)

$$T_e(\mathrm{h}) = T_0(\mathrm{h})\left[1 + \frac{1}{2}\left(\frac{91\,300}{T_0(\mathrm{h})} - 3\right) t^2(\mathrm{h})\right]$$

$$T_e(\mathrm{l}) = T_0(\mathrm{l})\left[1 + \frac{1}{2}\left(\frac{69\,000}{T_0(\mathrm{l})} - 3\right) t^2(\mathrm{l})\right]$$

Peimbert & Costero (1969)

t^2 y T_0

Te(h) and Te(l) are for the high – Te([OIII]) – and low – Te([NII]) – ionization zone

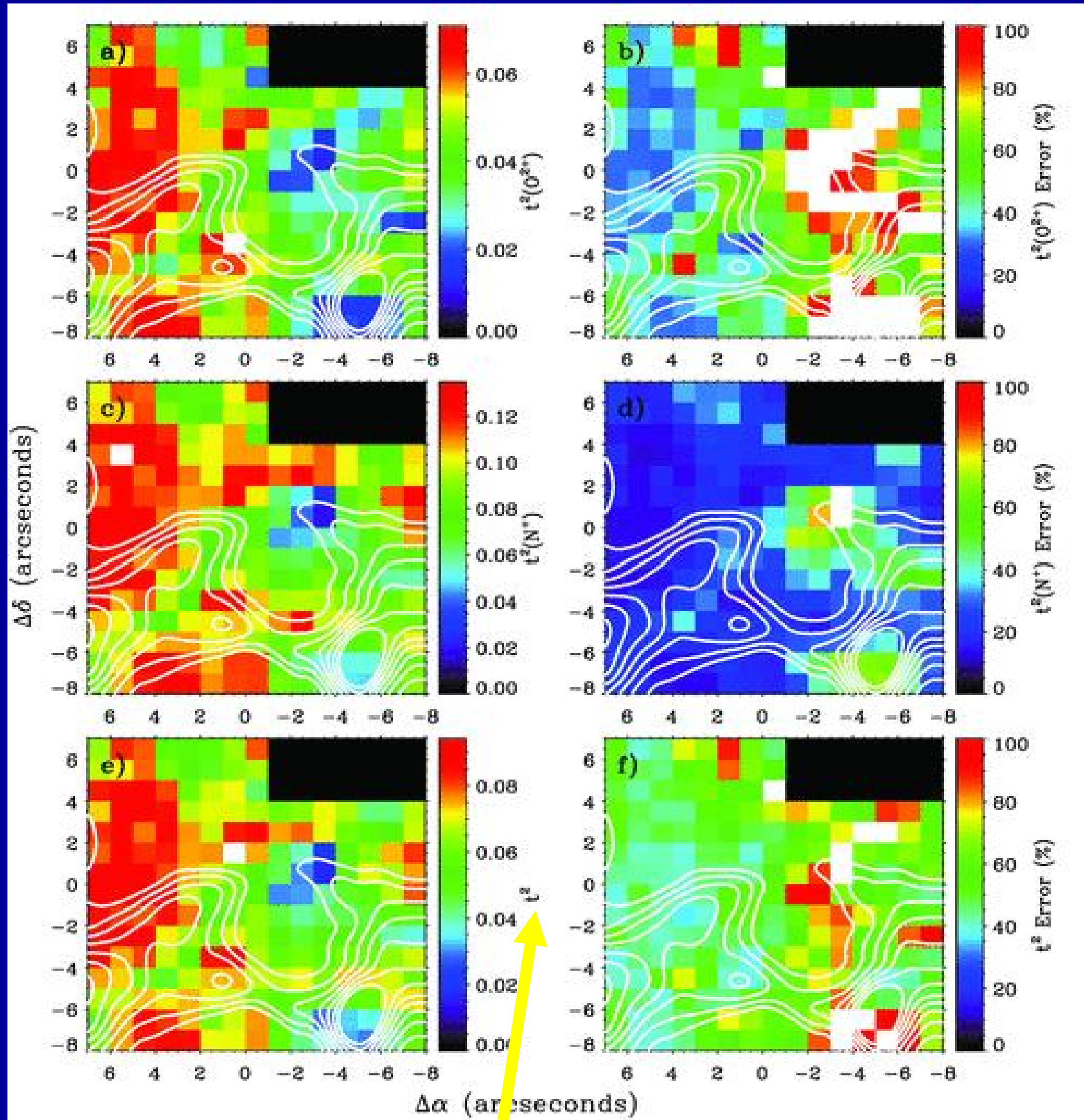

Eq (16) Peimbert, Peimbert & Luridiana (2002)

$\langle t^2 \rangle \sim 0.061 \pm 0.022$

HH objects in Orion: Results from PMAS

Correlations ADF and other nebular properties

ADF(O^{2+}), T_e , n_e , c (Hβ), t^2 and ionic abundances from CELs and RLs

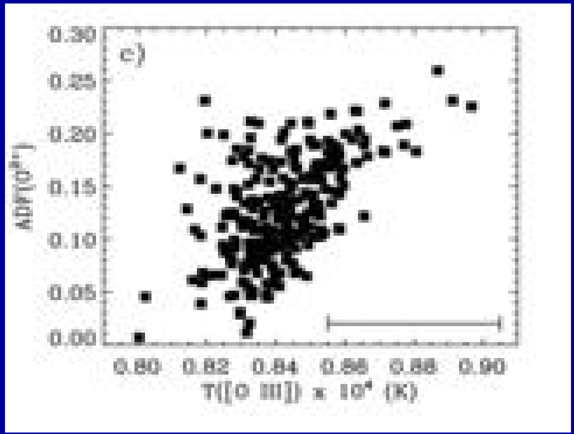

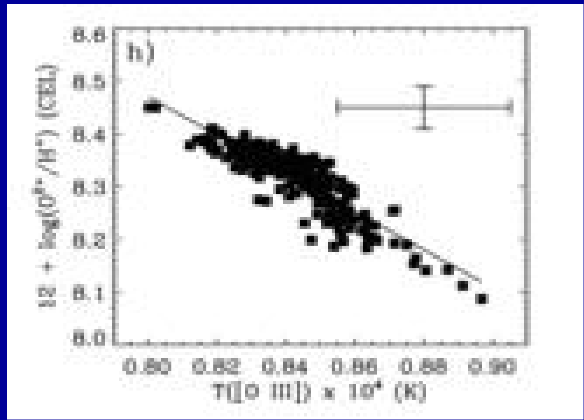

$$12 + \log\left(\frac{O^{2+}}{H^{+}}\right) = (11.4 \pm 0.1) + (-3.6 \pm 0.1)T_4$$

HH objects in Orion: Results from PMAS

Conclusions

- flux distributions of the [OIII] and OII lines are similar
- n_e ~4000 cm^{-3} in most FOV and ~10000 cm^{-3} at HH202-S and HH202-N
- T_e([OIII]) map shows a narrow range of variation (peak at HH202-S)
  T_e([NII]) shows larger variations and different spatial distribution
- We have obtained T_e(Bac) map, follows closely Te([OIII])
- O^+/H^+ ratio map highest values on the arc delineates north HH202, whereas the O^{2+}/H^+ shows an inverse behaviour (higher n_e shock gas)
- Spatial distributions of O^{2+} abundance from CELs and RLs agree in lower values at HH202-S, HH202-N and the arc connecting both, but values from RLs are always about 0.10 dex higher.
- t^2 map of the FOV from comparison T_e (Bac) and T_e → not match ADF map
  → AD and temperature fluctuations independent phenomena ???

HH objects in Orion: Results from PMAS

HH objects in Orion: Results from PMAS

Temperature fluctuations

2) Assuming ADF is produced by the presence of t^2

$$T_{\rm CEL} = T_0\left\{1+\left[\frac{(\Delta E_{\rm CEL}/kT_0)^2 - 3\Delta E_{\rm CEL}/kT_0 + 3/4}{\Delta E_{\rm CEL}/kT_0 - 1/2}\right]\frac{t^2}{2}\right\}$$

$$T_{\rm RL} = T_0\left[1-(1-\alpha)\frac{t^2}{2}\right]$$

$$T_{(4363/5007)} = T_0\left[1+\frac{1}{2}\left(\frac{91,300}{T_0}-3\right)t^2\right]$$

$$\left[\frac{N_{\rm CEL}(X^{+i})}{N_{\rm RL}(Y^{+j})}\right]_{t^2\neq 0.00} = \frac{T_{\rm RL}^{\alpha}T_{\rm CEL}^{0.5}}{T_{(4363/5007)}^{\alpha+0.5}} \times \exp\left[-\frac{\Delta E_{\rm CEL}}{kT_{(4363/5007)}}+\frac{\Delta E_{\rm CEL}}{kT_{\rm CEL}}\right] \times \left[\frac{N_{\rm CEL}(X^{+i})}{N_{\rm RL}(Y^{+j})}\right]_{t^2=0.00}, \quad (1$$

Peimbert et al. (2004)

~ spatial distribution ⇨ Not a genetic relatrionship between t^2 and ADF(O^{2+}) ??

$$T_{0,A} = \frac{\sum_j T_{e,j} n_{e,j}^2 [n(X^{+i})/n(H^+)]_j}{\sum_j n_{e,j}^2 [n(X^{+i})/n(H^+)]_j}$$

$$t_A^2 = \frac{\sum_j (T_{e,j}-T_{0,A})^2 n_{e,j}^2 [n(X^{+i})/n(H^+)]_j}{T_{0,A}^2 \sum_j n_{e,j}^2 [n(X^{+i})/n(H^+)]_j}$$

Mesa-Delgado et al. (2008)

t^2_A (O^{2+}) ~0.0004 t^2_A (N^+) ~0.0023

L. López-Martín